2021 43rd Annual International Conference of the
IEEE Engineering in Medicine & Biology Society (EMBC)
Oct 31 - Nov 4, 2021. Virtual Conference

Electric Field Comparison for TMS Using Different Neuroimaging Segmentation Methods

Tayeb A. Zaidi[1], Sergey N. Makarov[2,3], and Kyoko Fujimoto[1]

Abstract— **Computational electromagnetic modeling is a powerful technique to evaluate the effects of electrical stimulation of the human brain. The results of these simulations can vary depending on the specific segmentation of the head and brain generated from the patient images. Using an existing boundary element fast multipole method (BEM-FMM) electromagnetic solver, this work evaluates the electric field differences modeled using two neuroimaging segmentation methods. A transcranial magnetic stimulation (TMS) coil targeting both the primary motor cortex and the dorsolateral prefrontal cortex (DLPFC) was simulated. Average field differences along a 100 mm line from the coil were small (2% for motor cortex, 3% for DLPFC) and the average field differences in the regions directly surrounding the target stimulation point were 5% for the motor cortex and 2% for DLPFC. More studies evaluating different coils and other segmentation options may further improve the computational modeling for robust TMS treatment.**

Clinical relevance— **Patient-specific computational modeling will provide more information to clinicians for improved localization and targeting of neuromodulation therapies.**

I. INTRODUCTION

Magnetic and electrical brain stimulation therapies are a widely used method to treat neurodegenerative disorders. One of the commonly used non-invasive techniques is transcranial magnetic stimulation (TMS) that employs magnetic induction to stimulate the brain to improve symptoms for diseases such as depression. Computational modeling has been used to assess the efficacy and safety of TMS. A detailed brain model is available to allow for these assessments [1]; however, the model is only based on one subject. In order to allow for careful planning of a given treatment regimen, modeling needs to be completed on a per-patient basis.

A patient-specific brain model can be created using medical imaging data. Magnetic Resonance Imaging (MRI) is a commonly used structural imaging technique and there are a variety of semi-automatic segmentation methods available [2], [3], [4], [5] that can generate a 3D head model using a set of T_1- and T_2-weighted images. Segmentation varies across different methods [6], [7]. Therefore, it may affect electric field distributions in electric-field modeling [8].

In this study, we performed computational modeling of TMS with sixteen different patients targeting both the primary motor cortex and the dorsolateral prefrontal cortex (DLPFC). We then compare the electric fields from the two independent segmentation methods.

[1]Center for Devices and Radiological Health, US Food and Drug Administration, Silver Spring, MD 20993 USA
[2]Electrical & Computer Engineering Department, Worcester Polytechnic Institute, Worcester, MA 01609 USA
[3]A,A, Martinos Center for Biomedical Imaging, Massachusetts General Hospital, Boston MA 02115 USA

II. MATERIALS AND METHODS

A. MRI Data and Segmentation

MRI T_1- and T_2-weighted images were used from sixteen Human Connectome Project healthy subjects [9] with an isotropic resolution of 0.7 mm per voxel. Two pipelines within the SimNIBS software package v3.2 [10] were used for segmentation: *headreco* [11] and *mri2mesh* [12]. Both of these segmentation methods offer surface and volume segmentation of brain and head structures including gray matter (GM), white matter (WM), cerebrospinal fluid (CSF), skull, and skin.

The surface meshes were generated using the default options from SimNIBs for both segmentation methods. The default surface resolution yields surface meshes containing a combined total of roughly 800,000 facets.

B. Electromagnetic Simulation

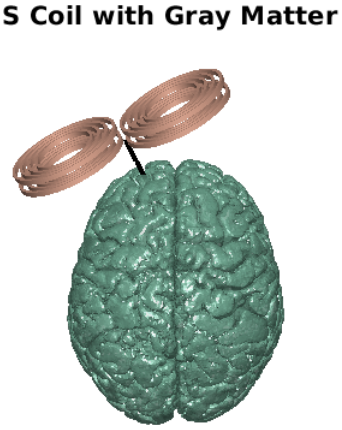

Fig. 1: An example placement of the TMS coil targeting the subject's left motor cortex is shown. The black line runs perpendicular to the coil and is used for electric field extraction.

A boundary element fast multipole method (BEM-FMM) solver was used for electromagnetic modeling [13]. The solver utilizes the generated surface meshes for field estimation. A figure-eight TMS coil was modeled with a diameter of 90 mm for each loop. The coil model was a replica of the commercial coil (MRiB91 of MagVenture). The coil was

placed to target both the patient's primary motor cortex (the hand knob) and the DLPFC via a projection approach and sulcus-aligned mapping. These regions were chosen because they are common targets for TMS therapy [14]. An example positioning of the coil is shown in Figure 1. The same set of two target points were used for each subject, located within the primary motor cortex and the DLPFC. The coil position was determined using three steps. First the coil was placed so that the centerline passed through the given target point on the gray matter interface. Second, the coil centerline was made to be perpendicular to the skin surface. Lastly the coil position was adjusted so that the dominant field direction was roughly perpendicular to the sulci.

C. Analysis

Average differences between mesh surfaces generated based on the *headreco* and *mri2mesh* segmentation were compared across the sixteen subjects for the gray matter, white matter and CSF surfaces. The electric field values were compared by extracting the values in a 100 mm line perpendicular to the TMS coil axis, along the black line shown in Figure 1. These values were extracted for both of the target points for each subject. The average electric field difference, maximum absolute difference, and maximum percentage difference were compared for all sixteen subjects. The average field difference at the target point for both the motor cortex and DLPFC was tested for statistical significance using a paired t-test.

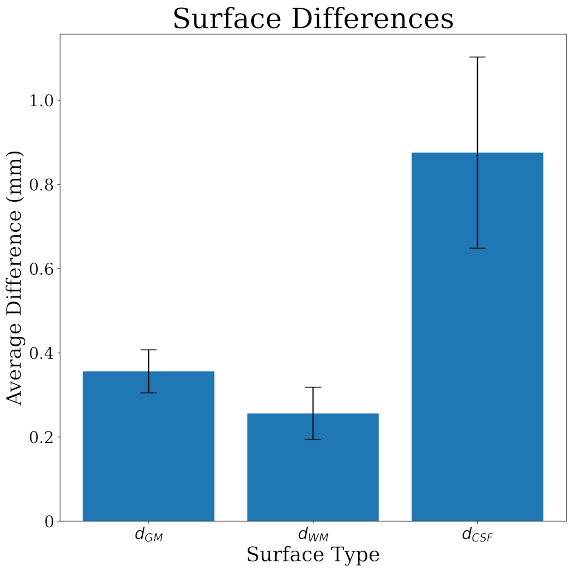

Fig. 2: Average distance between *headreco* and *mri2mesh* surfaces in millimeters across all 16 subjects for CSF, GM, and WM.

III. Results

The surfaces were successfully reconstructed using both segmentation methods. The average surface differences are summarized in Figure 2. Surface difference was calculated by taking the mean of the shortest distance from every triangle centroid of the relevant surface from one segmentation method to all triangle centroids of the surface from the other segmentation method. Average distances were only calculated for regions of the brain located in the superior cerebral cortex. The CSF surface difference was three times more than the white matter surface, with an average difference of 0.9 mm for the CSF and 0.3 mm for the white matter. All the surfaces are overlaid on a subject T_1-weighted image in Figure 3. The cortical thickness calculated from the *mri2mesh* method was thicker than that of the *headreco* method.

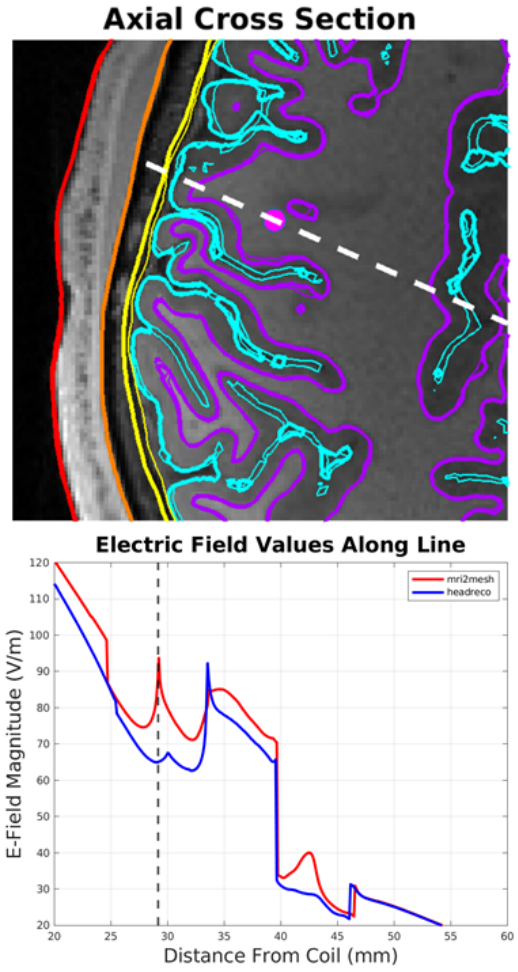

Fig. 3: Motor Cortex: Axial cross section of a subject with the target stimulation point in magenta. The thick contours show the *mri2mesh* field results and the thin contours show the *headreco* field results. Color indications for surfaces are red for skin, orange for skull, yellow for CSF, cyan for gray matter, and purple for white matter. The dotted white line on the axial cross section is a projection onto the XY plane of the 100mm line running along the axis perpendicular from the coil. The electric field result from the dotted white line was extracted as shown at the bottom of the figure. The dotted black line indicates the location of the target point of stimulation.

For the target point located in the motor cortex, the electric

TABLE I

Average percentage difference in the electric field for target points in the motor cortex and DLPFC for the 100 mm line and the average percentage difference in the region surrounding the target stimulation point (5 mm on either side). Average percentage difference ranges from 82% to 112%

Subject	1	2	3	4	5	6	7	8	9	10	11	12	13	14	15	16
Motor (All)	1.02	0.98	1.00	1.03	0.96	0.97	0.97	0.95	0.99	1.04	1.01	0.97	0.99	0.92	0.99	0.94
Motor (Target)	1.04	1.07	1.12	0.90	0.89	0.90	0.91	1.00	0.89	0.96	1.03	0.90	0.94	0.90	0.89	0.82
DLPFC (All)	0.97	1.08	1.07	0.95	1.03	1.00	1.01	1.08	1.12	1.04	1.04	1.06	1.01	1.03	0.99	0.96
DLPFC (Target)	0.94	0.98	1.03	0.95	1.05	0.99	0.92	0.93	1.11	1.09	1.00	1.01	0.96	0.92	0.91	0.95

fields showed similar distributions for both segmentation methods. There was an average difference in magnitude of 0.8 V/m and a maximum difference of 61 V/m. The percentage differences were 2% on average. In the region of interest within 5mm of the target point, the average percentage difference was approximately 5%.

For the target point located in the DLFPC, there was an average difference in value of 0.8 V/m and a maximum difference of 50 V/m. The percentage differences were 2.8% on average. In the region of interest within 5mm of the target point, the average percentage difference was approximately 1.8%.

The electric field difference across all 16 subjects at the target point between the two segmentation methods was statistically significant ($p = 0.004$) for the motor cortex. The electric field difference at the target point for the DLFPC was not significant ($p = 0.16$). The average percentage difference in the electric field for each subject and each target point is shown in Table I.

IV. Discussion and Conclusion

Comparison of the surface meshes from *mri2mesh* and *headreco* showed visible differences. The first difference in the surfaces can be seen at the CSF boundary, where the CSF surface was estimated consistently closer to the gray matter for the *headreco* segmentation. The cortical thickness for the *headreco* segmentation was also on average thinner. Such segmentation-dependent surface differences are in line with results shown in previous studies (cf., [15], [8]). In particular, Seiger et al. 2018 demonstrated that Freesurfer was more accurate in its calculation of cortical thickness however CAT12 based methods (such as *headreco*) were faster and yielded reliable results [16].

A comparison of the electric field values against the surface meshes shown in Figure 3 revealed that the electric field value was lower when the cortical thickness was thinner, as was the case for the *headreco* mesh. In both the motor cortex and the DLFPC, the low average percent difference in the electric field suggests that the effect of the segmentation method differences is minimal. Although the overall difference was low, the localized field difference near the target point across all 16 subjects was statistically significant for the motor cortex and could affect the intended stimulation there. The field difference for the DLFPC was not significant and the fields were qualitatively more similar between the two segmentation methods as shown in Figure 4.

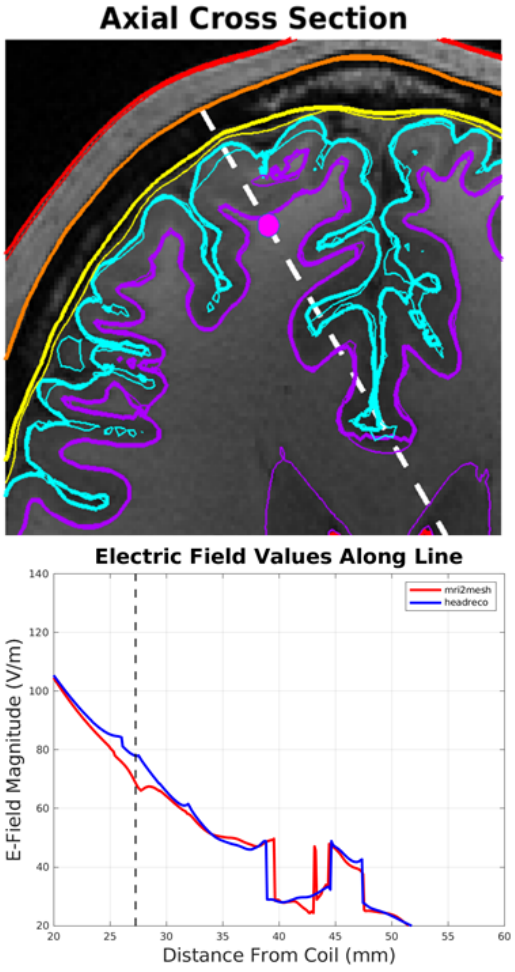

Fig. 4: DLPFC: Axial cross section of a subject with the target stimulation point in magenta. The thick contours show the *mri2mesh* field results and the thin contours show the *headreco* field results. Color indications for surfaces are red for skin, orange for skull, yellow for CSF, cyan for gray matter, and purple for white matter. The dotted white line on the axial cross section is a projection onto the XY plane of the 100mm line running along the axis perpendicular from the coil. The electric field result from the dotted white line was extracted as shown at the bottom of the figure. The dotted black line indicates the location of the target point of stimulation.

The percent difference in the electric field for the DLPFC was similar to that of the motor cortex along the entire 100 mm line for all sixteen subjects. However, the region directly surrounding the target point showed lower variability for the DLPFC target compared to the motor cortex. This can be seen in Figure 4 and is a also evident in the average percent difference in the 5 mm region surrounding the target point. This implies that there may be more surface variability in the motor cortex.

Analysis of the extracted electric field in Figure 3 showed sudden changes in the field from the *headreco* segmentation at a distance of 40 mm from the coil. This was not observed in the *mri2mesh* segmentation and is a result of the segmentation differences. For example, the *headreco* surface estimated sulci deeper compared to the *mri2mesh* surface in the region that the result was extracted. These sudden electric field changes resulting from segmentation differences can affect TMS therapy because the resulting neuronal excitation is a function of the electric field gradient rather than the electric field magnitude. Additional work that directly evaluates the gradient of the electric field will provide more insight into the effect of the segmentation on the TMS therapy.

Coil positioning was critical to the resulting electric field. In this study, coil positioning was determined automatically based on the topology of the input meshes used. The preprocessing steps to select the proper coil position may differ significantly between segmentations.

The resulting field differences for each coil position were small but measurable. Additionally the small field differences seen in average along the observation line are masking larger localized changes in the field of a larger percentage difference as shown in both Figure 3 and 4. This research demonstrates a need for patient-specific modeling considering that various previous studies have shown cortical thickness differences across age [17] and sex [18]. Future studies with different types of TMS coils and different segmentation methods may further improve computational modeling approach for robust treatment for TMS and other modalities.

DISCLAIMER

The mention of commercial products, their sources, or their use in connection with the material reported herein is not to be construed as either an actual or implied endorsement of such products by the Department of Health and Human Services.

ACKNOWLEDGMENT

The authors would like to thank William Wartman for his assistance in visualizing the segmentations. The authors would also like to thank Drs. Brian B. Beard and Sunder S. Rajan for their helpful feedback.

REFERENCES

[1] M. I. Iacono, E. Neufeld, E. Akinnagbe, K. Bower, J. Wolf, I. V. Oikonomidis, D. Sharma, B. Lloyd, B. J. Wilm, M. Wyss *et al.*, "MIDA: a Multimodal Imaging-Based Detailed Anatomical Model of the Human Head and Neck," *PloS one*, vol. 10, no. 4, p. e0124126, 2015.

[2] A. M. Dale, B. Fischl, and M. I. Sereno, "Cortical Surface-Based Analysis: I. Segmentation and Surface Reconstruction," *Neuroimage*, vol. 9, no. 2, pp. 179–194, 1999.

[3] B. Fischl, M. I. Sereno, and A. M. Dale, "Cortical Surface-Based Analysis: II: Inflation, Flattening, and a Surface-Based Coordinate System," *Neuroimage*, vol. 9, no. 2, pp. 195–207, 1999.

[4] Y. Zhang, M. Brady, and S. Smith, "Segmentation of Brain MR images Through a Hidden Markov Random Field Model and the Expectation-Maximization Algorithm," *IEEE Transactions on Medical Imaging*, vol. 20, no. 1, pp. 45–57, 2001.

[5] J. Ashburner and K. Friston, "Image segmentation," in *Human Brain Function*, 2nd ed., R. Frackowiak, K. Friston, C. Frith, R. Dolan, K. Friston, C. Price, S. Zeki, J. Ashburner, and W. Penny, Eds. Academic Press, 2003.

[6] K. Kazemi and N. Noorizadeh, "Quantitative Comparison of SPM, FSL, and Brainsuite for Brain MR Image Segmentation," *Journal of Biomedical Physics & Engineering*, vol. 4, no. 1, p. 13, 2014.

[7] D. L. Tudorascu, H. T. Karim, J. M. Maronge, L. Alhilali, S. Fakhran, H. J. Aizenstein, J. Muschelli, and C. M. Crainiceanu, "Reproducibility and Bias in Healthy Brain Segmentation: Comparison of Two Popular Neuroimaging Platforms," *Frontiers in Neuroscience*, vol. 10, p. 503, 2016.

[8] O. Puonti, G. B. Saturnino, K. H. Madsen, and A. Thielscher, "Value and Limitations of Intracranial Recordings for Validating Electric Field Modeling for Transcranial Brain Stimulation," *Neuroimage*, vol. 208, p. 116431, 2020.

[9] D. C. Van Essen, K. Ugurbil, E. Auerbach, D. Barch, T. E. Behrens, R. Bucholz, A. Chang, L. Chen, M. Corbetta, S. W. Curtiss *et al.*, "The Human Connectome Project: a Data Acquisition Perspective," *Neuroimage*, vol. 62, no. 4, pp. 2222–2231, 2012.

[10] G. Saturnino, A. Antunes, J. Stelzer, and A. Thielscher, "Simnibs: A Versatile Toolbox for Simulating Fields Generated by Transcranial Brain Stimulation," in *21st Annual Meeting of the Organization for Human Brain Mapping (OHBM 2015)*, 2015.

[11] J. D. Nielsen, K. H. Madsen, O. Puonti, H. R. Siebner, C. Bauer, C. G. Madsen, G. B. Saturnino, and A. Thielscher, "Automatic Skull Segmentation from MR Images for Realistic Volume Conductor Models of the Head: Assessment of the state-of-the-art," *Neuroimage*, vol. 174, pp. 587–598, 2018.

[12] M. Windhoff, A. Opitz, and A. Thielscher, "Electric Field Calculations in Brain Stimulation based on Finite Elements: An Optimized Processing Pipeline for the Generation and Usage of Accurate Individual Head Models," Wiley Online Library, Tech. Rep., 2013.

[13] S. N. Makarov, W. A. Wartman, M. Daneshzand, K. Fujimoto, T. Raij, and A. Nummenmaa, "A Software Toolkit for TMS Electric-field Modeling with Boundary Element Fast Multipole Method: An Efficient MATLAB Implementation," *Journal of Neural Engineering*, vol. 17, no. 4, p. 046023, 2020.

[14] E. Raffin, G. Pellegrino, V. Di Lazzaro, A. Thielscher, and H. R. Siebner, "Bringing transcranial mapping into shape: Sulcus-aligned mapping captures motor somatotopy in human primary motor hand area," *NeuroImage*, vol. 120, pp. 164–175, 2015. [Online]. Available: https://www.sciencedirect.com/science/article/pii/S1053811915006333

[15] R. Righart, P. Schmidt, R. Dahnke, V. Biberacher, A. Beer, D. Buck, B. Hemmer, J. Kirschke, C. Zimmer, C. Gaser *et al.*, "Volume Versus Surface-Based Cortical Thickness Measurements: A Comparative Study with Healthy Controls and Multiple Sclerosis Patients," *PLoS One*, vol. 12, no. 7, p. e0179590, 2017.

[16] R. Seiger, S. Ganger, G. S. Kranz, A. Hahn, and R. Lanzenberger, "Cortical Thickness Estimations of FreeSurfer and the CAT12 toolbox in Patients with Alzheimer's Disease and Healthy Controls," *Journal of Neuroimaging*, vol. 28, no. 5, pp. 515–523, 2018.

[17] D. H. Salat, R. L. Buckner, A. Z. Snyder, D. N. Greve, R. S. Desikan, E. Busa, J. C. Morris, A. M. Dale, and B. Fischl, "Thinning of the Cerebral Cortex in Aging," *Cerebral Cortex*, vol. 14, no. 7, pp. 721–730, 2004.

[18] E. R. Sowell, B. S. Peterson, E. Kan, R. P. Woods, J. Yoshii, R. Bansal, D. Xu, H. Zhu, P. M. Thompson, and A. W. Toga, "Sex Differences in Cortical Thickness Mapped in 176 Healthy Individuals Between 7 and 87 years of Age," *Cerebral Cortex*, vol. 17, no. 7, pp. 1550–1560, 2007.